DOI: 10.13009/EUCASS2019-254

Combined experimental and calculation method for sonic boom investigation

*Tatiana Kiseleva**
* *Khristianovich Institute of Theoretical and Applied Mechanics, Siberian Branch of Russian Academy of Sciences, Institutskaya St. 4/1, Novosibirsk, 630090, Russia*
**Novosibirsk State University,*
Pirogova St. 2, Novosibirsk, 630090, Russia
bobarykina@ngs.ru

Abstract
Sonic boom is one of the main problems in the creation of a supersonic passenger aircraft. The main problem of sonic boom modelling is the large extent of the area under investigation, where the perturbed pressure levels vary by several orders of magnitude. Paper describes the combined experimental and computational approach of the sonic boom modelling. Some results obtained using the method are shown.

1. Introduction

Supersonic flight is a new quality of aviation mobility. The one-day travel zone for subsonic aircraft is limited to a distance of 3500 km. The supersonic airplane expands the one-day trip zone to 7500 km and more than halves the flight time. Creation of a supersonic civil aircraft faces the environmental and economic restrictions critical for the aircraft operation right and marketability [1]. Environmental restrictions mean the acceptable noise level on the ground, reduction of hazardous atmospheric exhaust, and acceptable sonic boom (SB) formed by a heavy aircraft flying at supersonic speeds.
Near the supersonic aircraft there are intermediate SW, plus rarefaction and compression waves created by individual elements of the aircraft. As non-linear effects (speed of disturbance propagation versus the disturbance amplitude) propagate in the atmosphere, the flow pattern transforms in the N-profile of the disturbed pressure wave which is referred to as the “N-wave” of the sonic boom. Suddenness and short duration of the N-wave action are perceived negatively by humans and alive creatures. People undergoing periodical action of the sonic boom may suffer from psychological and physiological diseases [2]; animals may change the habitat, etc. Today, the supersonic overland missions are prohibited both in the USA and Europe. In Russia, the pressure drop at the SB wave of 90 Pa ± 20 Pa was introduced in the State Standard (GOST) 23552-79 1979 as an optional value. Note that, during the cruise-altitude flights of Tu-144, the level sonic boom correlated to the prescribed value. Nowadays, the International Civil Aircraft Organization (ICAO) is developing the standards for the sonic boom level acceptable for humans.
The aircraft SB level depends on the aircraft shape, size, real atmosphere conditions, local relief, etc. Contradictory requirements to the configuration make it difficult to create an environmentally friendly aircraft with the acceptable sonic boom level which would have the high aerodynamic quality and hence the marketability. This is especially important for heavy aircrafts (above 1000 kN), which is caused by the increased contribution of the lifting force in the sonic boom rising along with the aircraft weight.

2. Methods of the sonic boom investigations

The main problem of SB modelling is the large extent of the area under investigation, where the perturbed pressure levels vary by several orders of magnitude.
Normally, the sonic boom phenomenon is studied in the near and far fields [3]. The near field of the SB adjoins the aircraft and has a complicated flow structure with shock waves, rarefaction and compression waves; its length is about the aircraft length ($K = H/L \sim L$, where H is the height distance from the aircraft, L is its characteristic size). The length of the far field where the sonic boom parameters vary feasibly in accordance with the asymptotic law, realizes within the distances of $K \sim L^2$. The middle zone of the SB is an intermediate one between the near and far

DOI: 10.13009/EUCASS2019-254

fields and features the presence of intermediate shock waves on the pressure profile of the sonic boom wave; these waves are generated by the main elements of the aircraft configuration, for example, from a wing or nacelles.
There are various approaches to the study of the SB phenomenon:

- Flight (full-scale) tests;
- Experimental simulation of the SB phenomenon in aeroballistics installations, in wind tunnels of short-term or periodic action;
- Calculation methods.

Flight tests are the most informative and reliable [4], but extremely complex and expensive. Numerical simulation is the most acceptable way to modelling the problem. However, numerical modelling is the main research method [5], but it requires huge computational capability, the construction of complex grids to describe aircraft configurations, and, in addition, contains some assumptions. In this context, the numerical modelling of the sonic boom phenomenon should be added by experimental investigations purposed to obtain reliable information for the bodies of arbitrary configuration, and to validate the results of numerical calculations. Wind tunnels are commonly used to perform the physical simulation of the sonic boom wave formation and propagation. The fundamental task of the interaction, propagation, and methods of diagnostics of weak shock waves in the near field of the flow can be considered with the aid of wind tunnels.
In ITAM SB RAS, under the supervision of Academician V. V. Struminskij, the combined experimental and computational approach has been developed to model the sonic boom effect [6]. The experimental part of the method is based on the modelling of the near field of the sonic boom in small-size wind tunnels with large models. Nowadays experimental simulation in this method is alternated/added with computational one [6]. At the first stage, the numerical methods were applied to solve the task of the supersonic flow around the configuration at the assigned Mach number and angle of attack. By the results of the numerical solution of this task, the aerodynamic characteristics and parameters of the disturbed flow are detected on the control surface within the assigned distance from the body axis. Evolution of the measured/calculated data of the disturbed pressure propagating over long distances is determined by the computational methods based on the quasi-linear theory [7].

3. Near field modelling

3.1 Experimental modeling

Fig. 1 shows the experiment schematic. The investigations were carried out in the wind tunnel T-313 on the following modes: Mach number M = 2.04, unit Reynolds number of the incoming flow Re1 = (15-25)*106, total temperature T0 = 283 K. The dimensions of the rectangular section of the working part were 0.6 × 0.6 × 2 m.

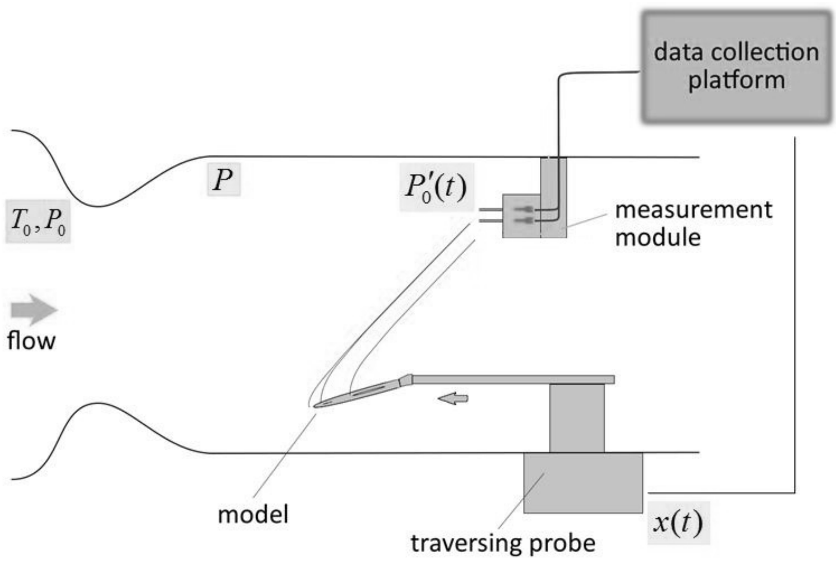

Figure 1: Experimental scheme

The model coordinator is installed on the bottom wall of the working part in the wind tunnel. On the coordinator driver shaft there is a sensor of model motion along the lengthwise coordinate *x(t)* (Fig. 1). On the upper wall of the working part there is a pylon on which the removable measurement unit is fastened; in this unit there are the measurement probes of full pressure behind the normal shock wave (the Pitot tubes).

DOI: 10.13009/EUCASS2019-254

Strain pressure gages D1, D2, typeТДМ-А-0,16 with the rated pressure of 0.16 MPa were used in the experiments. The calibration tests showed that the maximum deviation did not exceed 6 Pa.
Measured signals through the automated switching system HP34970A entered the 45-channel recording multimeter, registering 5.5 decimal places with an error of 0.004%, followed by the transfer of digital information to the PC for writing to the database and subsequent processing.
During the experiment, the model fastened with the aid of a tail holder on the model coordinator, was permanently moved with the assigned speed in the lengthwise direction windward the flow in respect to the immovable measurement probe. During this process, the discrete readings of six gages (D1 – D6) were registered with the assigned time step (about 400 ms) or coordinate pitch (about 0.5 mm at the movement speed of 1.3 mm/s)). The profile of the disturbed static pressure is detected from the arrays of the measured values from three gages (D2 (or D1), D3, D4), which after the primary processing correspond to: the absolute disturbed pressures behind the normal shock wave – the gage D2 or D1, the absolute full pressure of the flow – the gage D4, and the lengthwise coordinates at which the readings are counted – the gage D3.
Recorded during the experiment parameters and the corresponding sensors are listed in the Table 1.

Table 1: Measured parameters and corresponding gage numbers

Gage number	**Parameter**	**Unit**
D1	P_0’	Pa
D2	P_0’	Pa
D3	x	mm
D4	P	Pa
D5	T_0	K
D6	P_0	Pa

3.2. The model

The investigations were carried out with the model shaped as a tandem of two wings on the fuselage. The general view of the model is shown in Fig. 2.

Figure 2: Photo of the model

The fuselage length is L = 140 mm, its maximal diameter corresponding to the cylindrical parts is d_m = 10.7 mm. The canard wing geometrically similar to the main one was installed within the distance of the side chord start from the fuselage nose of 27.5 mm. The area of the canard wing was 10% of the total wings area.
The model was fixed on the coordinator shaft under the angle of attach of 3.5o. The true angle of attack of the model in the supersonic flow might reach $\alpha = 5^o$, the holder deformation from the transversal loading is taken into account.

4. Far field modelling

The solution of equations describing the propagation of a nonstationary Riemann wave was obtained at an arbitrary distance r from the original profile using the quasilinear theory [7]. The equations determining the magnitude of the

DOI: 10.13009/EUCASS2019-254

perturbed pressure on the characteristic and the position of this characteristic at an arbitrary distance from the original profile, in the first approximation with respect to the intensity of perturbations, have the following forms:

$$\Delta\overline{p} = \Delta\overline{p}_0 \left(\frac{r_0}{r}\right)^{1/2} \quad \textbf{(1)}$$

$$x = \beta r - k_1 \Delta\overline{p} r_0^{1/2} \left(r^{1/2} - r_0^{1/2}\right) + x_0 \quad \textbf{(2)}$$

$\Delta\overline{p} = \frac{p - p_\infty}{p_\infty}$ - relative overpressure, $\beta = \sqrt{M_\infty^2 - 1}$, M - Mach number, $k_1 = \frac{(\gamma+1)M_\infty^2}{\gamma\beta}$, γ - ratio of specific heat.

Equation (2) in the second approximation is determined:

$$x = \beta r - k_1 \Delta\overline{p} r_0^{1/2} \left(r^{1/2} - r_0^{1/2}\right) + k_2 \Delta\overline{p}^2 r_0 \ln\left(\frac{r}{r_0}\right) + x_0 \quad \textbf{(3)}$$

where $k_2 = \frac{(\gamma+1)^2 M_\infty^2}{2\gamma\beta^{1/2}}$.

The shock wave position in the deformed profile was determined from the condition of equality of the pulses of the ambiguous and corrected profile.

5. Some results and discussion

Figure 3 presents the results of measurement of the full pressure profiles behind the normal shock waves generated by the model. During the initial motion of the model in respect to the measurement probes, the effect of the head SW on the probe readings was excluded. These data were taken as the full pressure behind the normal shock wave in the undisturbed flow $\Delta p'_{0\infty}$. The first pressure peak corresponds to the shock wave from the model nose. The second peak of pressure corresponds to the shock wave from the wing. Tail shock wave is not modelled due to model strut. The expanding part of the model strut causes a compression wave in the final section of the profile.

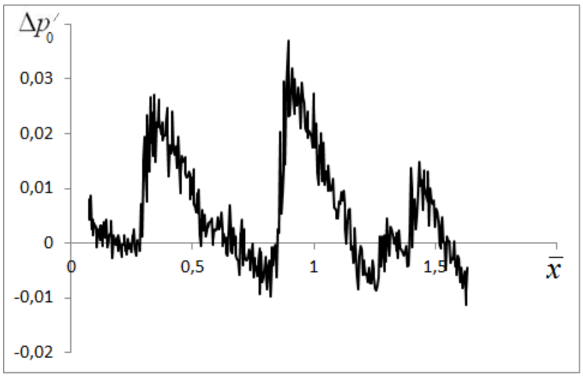

Figure 3: The full pressure behind a direct shock wave (Pitot pressure) signatures

Every linear value is referred to the fuselage length L, i.e. are presented in calibers: K = H/L is the relative distancing (transversal) of the model from the measurement probe, $\overline{x} = x/L$ is the relative lengthwise coordinate of the disturbed parameters profile.

The coordinate beginning (x = 0 mm) corresponds to the initial point of the model motion. The pressure profiles measured by the pressure gage D1 correlate to the distance K = H/L = 1.43 (1), where H is the distance from the model nose to the measurement probe, L = 140 mm is the model length.

DOI: 10.13009/EUCASS2019-254

The profiles include: the head and intermediate shock waves and the compression wave formed by the shock waves from the fuselage nose, wing, and expanding part of the model holder, respectively.
Figure 4. shows the excessive static profiles pressure versus the relative coordinate calculated from the initial data in the isentropic ratios.

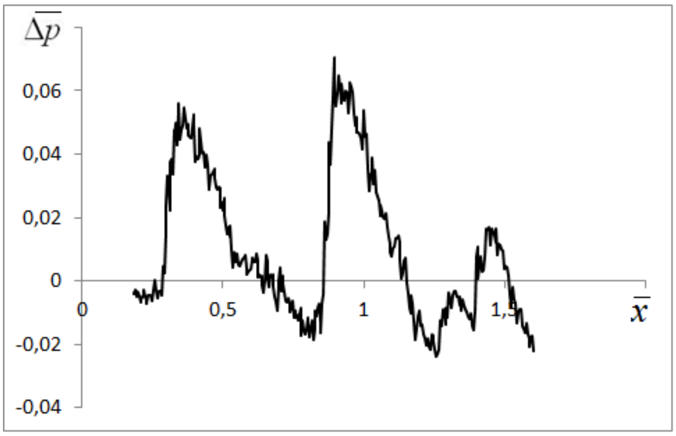

Figure 4: The relative excess static pressure as a function of normalized coordinate

Results of the profile (Fig. 4) expansion of the over long distances by the computational method are shown on the Fig. 5. Results are shown for K = 20. We can see the bow shock wave, intermediate shock wave from the wing and tail shock wave. The head shock wave and the intermediate shock wave do not interact and the N-wave, specific of sonic boom, is not realized. Due to the absence of a shock wave in the tail section of the experimental profile, the closing shock wave (dash line) was added to the calculation from experiments with another model strut.

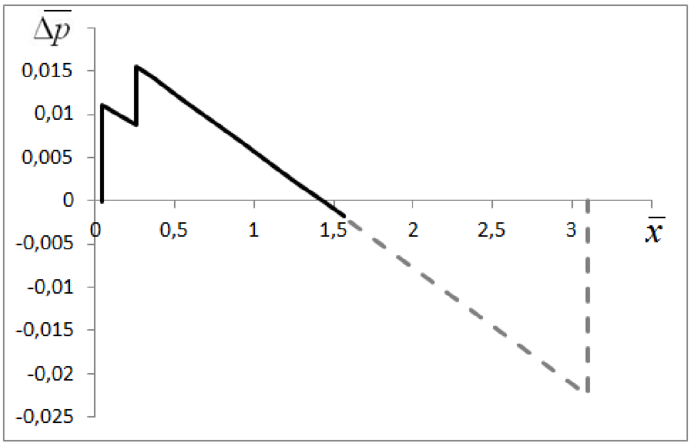

Figure 5: Sonic boom far field signature

5. Conclusions

New supersonic passenger aircraft must have a low sonic boom level. The large extent of the area under investigation and high perturbed pressure levels variation of magnitude are the main problem of modelling the phenomenon.
The combined experimental and computational approach of the sonic boom modelling is described. The sonic boom phenomenon is studied in the near and far fields. The experimental part of the method is based on the modelling of the near field of the sonic boom in wind tunnel. Evolution of the measured/calculated data of the disturbed pressure propagating over long distances is determined by the computational methods based on the quasi-linear theory. Some results obtained using the method are shown.

Acknowledgments

The research was carried out within the framework of the Program of Fundamental Scientific Research of the state academies of sciences in 2013-2020 (project No. AAAA-A17-117030610121-9)

References

[1] Chernyshev, S. L., Lyapunov, S. V., and Wolkov A. V. 2019. Modern problems of aircraft aerodynamics, *Advances in Aerodynamics*, 1:7.

[2] Rylander, R. 2004. Physiological aspects of noise-induced stress and annoyance. *Journal of Sound and Vibration*. 277 : 471-478.

[3] Ma, B., Wang, G., Ren, J., Ye, Zh., and Zha, G. 2017. Near Field Sonic Boom Analysis with HUNS3D Solver. *AIAA 2017* : 0038.

[4] Kanamori, M., Takahashi, T., Makino, Yo., Naka, Yu., and Ishikawa, H. 2018. Comparison of Simulated Sonic Boom in Stratified Atmosphere with Flight Test Measurements. *AIAA Journal* 56 (7) :2743-2755.

[5] Morgenstem, J. M. How to accurately measure low sonic boom or model surface pressures in supersonic wind tunnels. *AIAA* 2012 :3215.

[6] Fomin, V. M., Chirkashenko, V. F., Volkov, V. F., and Kharitonov, A. M. 2011. Effect of the supersonic transport configuration on the sonic boom parameters. *Thermophys. Aeromech.* 18: 509–522.

[7] Whitham, G.B. The flow pattern of a supersonic projectile. *Comm. Pure Appl. Math.* 5:301-338.